

HOSTED BY



Contents lists available at ScienceDirect

Journal of King Saud University – Science

journal homepage: [www.sciencedirect.com](http://www.sciencedirect.com)

Original article

## Potential anticancer agents identification of *Hystrix brachyura* bezoar through gas chromatography-mass spectrometry-based metabolomics and protein-ligand interaction with molecular docking analyses



Al'aina Yuhainis Firus Khan<sup>a,b,\*</sup>, Ridhwan Abdul Wahab<sup>c</sup>, Qamar Uddin Ahmed<sup>d</sup>, Alfi Khatib<sup>d</sup>, Zalikha Ibrahim<sup>d</sup>, Tanzina Sharmin Nipun<sup>e</sup>, Hapizah Nawawi<sup>b</sup>, Syed Najmul Hejaz Azmi<sup>f</sup>, Md. Zaidul Islam Sarker<sup>g</sup>, Zainul Amiruddin Zakaria<sup>h</sup>, Saad Alkahtani<sup>i</sup>, Abdullah A. Alkahtane<sup>i</sup>

<sup>a</sup> Department of Science Education, Faculty of Education, Universiti Teknologi MARA, Puncak Alam, Malaysia

<sup>b</sup> Institute for Pathology, Laboratory and Forensic Medicine (I-PPerForM), Universiti Teknologi MARA, Sungai Buloh, Malaysia

<sup>c</sup> Department of Preclinical, International Medical School, Management and Science University, Shah Alam, Malaysia

<sup>d</sup> Drug Discovery and Synthetic Chemistry Research Group, Department of Pharmaceutical Chemistry, Kulliyah of Pharmacy, International Islamic University Malaysia, 25200 Kuantan, Pahang DM, Malaysia

<sup>e</sup> Department of Pharmacy, Faculty of Biological Sciences, University of Chittagong, Chittagong, Bangladesh

<sup>f</sup> Applied Sciences Department (Chemistry Section), Higher College of Technology, University of Technology and Applied Sciences, P. O. Box 74, Al-Khuwair-133, Muscat, Sultanate of Oman

<sup>g</sup> Cooperative Research, Extension and Education Services (CREES), Northern Marianas College, Saipan, MP 96950, USA

<sup>h</sup> Borneo Research on Algesia, Inflammation and Neurodegeneration (BRAIN) Group, Department of Biomedical Sciences, Faculty of Medicines and Health Sciences, University Malaysia Sabah, Jalan UMS, Kota Kinabalu 88400, Sabah, Malaysia

<sup>i</sup> Department of Zoology, College of Science, King Saud University, P. O. Box 2455, Riyadh 11451, Saudi Arabia

### ARTICLE INFO

#### Article history:

Received 15 March 2023

Revised 30 March 2023

Accepted 22 May 2023

Available online 26 May 2023

#### Keywords:

*Hystrix brachyura*

GC-MS

Metabolomics

Molecular docking

Bcl-2

Cyclin B/CDK1

### ABSTRACT

**Background:** Bezoar (PB) is a rare, solidified form of undigested food commonly found in the gastrointestinal tract of porcupine (*Hystrix brachyura*). It is believed to be traditionally used to treat various diseases including different kinds of cancers in Malaysia. However, its active principles have not been found out yet. The purpose of this study was to investigate the anticancer property of PB extract as well as to identify the metabolites responsible for its anticancer effect through a widely acclaimed metabolomics approach.

**Methods:** Initially, 25 PB extracts using various solvent ratios of methanol–water (100, 75, 50, 25, 0% v/v) were prepared in regard to metabolomics approach and subsequently the cytotoxicity of each extract was determined against (melanoma) A375 cell line. The metabolites profiling of the most potent extract was conducted using gas chromatography mass spectrometry (GC-MS) and *in silico* investigation was performed on Bcl-2 and cyclin/CDK1 complex protein.

**Results:** The correlation of the bioactivity with GC-MS data produced an orthogonal partial least square (OPLS) model which pinpointed four putative active compounds namely (1) cholest-7-en-3-beta-ol,4,4-dimethyl-,acetate; (2) 4-androsten-4-ol-3,17-dione; (3) isolongifolol and (4) gallic acid. The *in silico* data suggested the binding score and binding mode of active metabolites with the amino acid residues of protein via hydrophobic interactions.

**Conclusion:** This study is the first to report the identified anticancer compounds from PB extract and evaluate them using molecular docking. This further confirms and justifies its traditional usage as an alternative medicine for the treatment of cancer in Malaysia.

© 2023 The Author(s). Published by Elsevier B.V. on behalf of King Saud University. This is an open access article under the CC BY-NC-ND license (<http://creativecommons.org/licenses/by-nc-nd/4.0/>).

\* Corresponding author at: Department of Science Education, Faculty of Education, Universiti Teknologi MARA, Puncak Alam, Malaysia.

E-mail address: [yuhainis@uitm.edu.my](mailto:yuhainis@uitm.edu.my) (A.Y. Firus Khan).

Peer review under responsibility of King Saud University. Production and hosting by Elsevier.



Production and hosting by Elsevier

## 1. Introduction

*Hystrix brachyura* is Malayan porcupine part of *Hystricidae* family, a common species found in Southeast Asian land (Lim & Wang, 2016). The population of *H. brachyura* had drastically reduced from January 1998 to January 2008, according to the International Union for Conservation of Nature (IUCN) red list and was thus categorized as a vulnerable species (Lunde et al., 2008). The focal reason of rapid decrease in population was due to higher demand for meat and bezoars by the people/traditional practitioners (Azliza et al., 2012). Bezoars are undigested food materials that are calcified in the animal's gastrointestinal tract and not eliminated from the body (Barroso, 2014). Bezoars were believed to be widely used as animal-based remedies to treat all kinds of deadly diseases or illnesses previously as revealed by different ethnopharmacological surveys to reveal traditional uses. Among the diseases reported treated by bezoars are intestinal worms, kidney stones, malignant diseases, cholera, quartan fevers, plague, acute febrile illness, measles, smallpox, bilious, pleurisy, intestinal obstructions, palpitations of the heart, jaundice, heart diseases, the bloody flux, epilepsy, internal abscesses, chicken pox fevers and leprosy (Barroso, 2017; Duffin, 2013).

In Malaysia, PB has been used for its antioxidant, anti-dengue, and anticancer properties. A study carried out in 2018 to ascertain its antioxidant potential reported three types of PB namely grassy PB, black PB and powdery PB exhibit antioxidant effects which were evaluated through *in vitro* ferric reducing power (FRP), free radical scavenging (FRS), reactive nitrogen species (RNS), reactive oxygen species (ROS) and nitric oxide (NO) assays. In another study performed by us, different grassy PB exhibited anticancer activity by inhibiting A375 cancer cells in time and dose-dependent manner, induced apoptosis via intrinsic pathway, arrested cells in G2 phase, inhibited angiogenesis and metastasis (Firus Khan et al., 2019a,b).

The usage of PB is impractical in the long run as the process of obtaining PB is through the sacrifice of the porcupine which can threaten the extinction of *H. brachyura*. Furthermore, the phytobezoars differ in colour, shape, texture and quality depending on the type of food consumed by the porcupine and duration of time the bezoar remains in the body of the porcupine. The bezoar varies in size, the longer the bezoar duration (years) in porcupine's body, the higher the weight of it is produced including the effect on colour and texture change, thereby grassy bezoar is eventually transformed to hardened rock over time (Duffin, 2013). Each porcupine bezoar found is unique and distinct to another, hence the composition of each bezoar varies, and it is impossible to standardize the bezoars for medicinal purposes. Therefore, the feasible option to solve the issues is by identifying the bioactive compounds of the bezoar. As a matter of fact, the PB is generally obtained in a very small size and quantity, therefore isolation of bioactive compounds is a strenuous and challenging task.

Present study has taken the metabolomics approach into account to identify the putative active compounds present in bezoar as anticancer agents. In this approach, the gas chromatography-mass spectrometry was correlated with the bioactivity data on A375 cells (median inhibition concentration) analyses using multivariate data analysis (MVDA) (Manier et al., 2019). This study also presents the molecular interaction between targeted protein (Bcl-2 and cyclin B/CDK1 complex) and the inhibitors (ligand) identified from PB extracts through gas chromatography mass spectrometry technique. The *in-silico* study was performed to model the putative ligand-receptor complex formed by representing the binding affinities and catalytic pocket of the identified tentative active compounds.

## 2. Materials and methods

### 2.1. Materials and chemicals

According to Malaysian law, the *H. brachyura* is a secured animal. The Malaysian government's Department of Wildlife and National Parks (JPHL&TN (IP): 100–34/1.24 Jld 8) approved the use of PB for research purposes. Bezoar was directly purchased from the aborigine's people, the only group of people who are allowed (possessing licence) to hunt porcupine in Malaysia for medicinal purposes. Human melanoma, A375 cells was acquired from the American Type Culture Collection (ATCC), USA. The A375 cells were grown in complete media with 89% Dulbecco's modified Eagle medium, 10% fetal bovine serum (FBS) and 1% antibiotic of penicillin–streptomycin from Nacalai Tesque, Japan. Phosphate buffer saline (PBS) obtained from Gibco, USA was used for cell washing and standard anticancer drug, fluorouracil (5-FU) from Sigma, USA was used as positive control. Cytotoxicity assay used MTS cell proliferation assay from Promega, USA. Analytical grade methanol used for the extraction was purchased from Merck, Germany while chemicals used for derivatization viz. methoxyamine hydrochloride, pyridine and N-methyl-N-(trimethylsilyl)-tri fluoroacetamide were obtained from Sigma Aldrich, USA.

### 2.2. Porcupine bezoar extract preparation for metabolomics

The PB was crushed using a mortar pestle into fine powder. 300 mg of PB powder was sonicated through an ultrasonication process for 30 min using 100% water (A), 75% water: methanol (B), 50% water: methanol (C), 25% water: methanol (D) and 100 % methanol (E) as solvents. The resultant extract's filtrates were filtered using Whatman filter paper and then oven-dried (40 °C) to remove residual solvents. The extracts for each solvent (ratio) were prepared in 5 replicates and kept at –80 °C in the deep chiller until further analysis.

### 2.3. Derivatization of sample

The derivatization step was prepared as reported previously (Murugesu et al., 2018). The derivatization step was performed to increase the compound's volatility by modifying the functional group. Initially, 50 µL of pyridine was used as a solvent to dissolve 25 mg PB extract by sonicating it for 2 min to ensure the extract was completely dissolved. The mixture was then vortexed with 100 µL of methoxyamine hydrochloride (20 mg/mL in pyridine) before being incubated for 2 h at 60 °C in an incubator shaker. Afterward, the mixture we mixed with 300 µL of N-Methyl-N-(trimethylsilyl) trifluoroacetamide (MSTFA) before incubating for another 30 min. The derivatized extract was filtered and kept in dark overnight at room temperature prior to injecting into the GCMS machine.

### 2.4. Cytotoxicity of porcupine bezoar extracts on A375 cells

All extracts were subjected to cytotoxicity assay on melanoma cells namely A375. The assay measured median inhibitory concentration (IC<sub>50</sub>) by following MTS kit as recommended by the manufacturer upon 72 h exposure as described previously (Firus Khan et al., 2019a). Anticancer drug, Fluorouracil (5-FU) was used as control in the study as positive control. The IC<sub>50</sub> values for all extracts were analysed using GraphPad Prism software.

## 2.5. Gas chromatography mass spectrometer (GC–MS) analysis

All samples were analysed with an Agilent 6890 GC–MS (Agilent Technologies, USA) connected to an HP 5973 mass selective detector (Agilent Technologies, USA). DB-5MS column was used for this experiment, which had 0.25 mm film thicknesses and a 250 mm inner diameter. The initial temperature was 85 °C, then set to increase slowly at a rate of 2 °C/minute to 315 °C with 5 min hold time. A continuous flow rate of 1.0 mL/min was maintained where helium was used as the carrier gas, with an injection volume of 1 µL and a 10:1 ratio as the inlet mode of split. The spectra were compared with the National Institute of Standards and Technology (NIST14) database. The chromatogram and mass spectra were processed using Advanced Chemistry Development lab (ACD) software and the raw data were converted into CDF format file. MVDA was performed utilizing the SIMCA-P<sup>+</sup> 14.0 program with observation of 25 sample spectra and one dependent variable (IC<sub>50</sub>). Using the metabolomics approach, active compounds detected from GCMS were predicted and putative in nature.

## 2.6. Molecular docking analysis

Our previous study reported for PB extract that it exerted cytotoxicity by inducing apoptosis and arresting cells in G2 phase (Firus Khan et al., 2019a,b). *In silico* study was performed to analyse the putative active compounds detected from GC–MS with target proteins namely Bcl-2 and cyclin B/CDK1 interaction. The three-dimensional (3D) structures of ligands were acquired from PubChem database (National Centre for Biotechnology Information (NCBI) in SDF format and Avogadro software was used to convert the SDF to PDB format. Gasteiger charges were added while ligands were prepared, rotatable bonds and torsion were assigned onto the structures using AutoDock Vina 1.1.2 software. The crystallographic structure of proteins related to anticancer activity viz. Human anti-apoptosis Bcl-2 (PDB ID: 2W3L) and human G2 phase arrest cyclin B/CDK1 complex (PDB ID: 6GU2) were collected from Protein Data Bank (PDB) of *Homo sapiens* species. Only the proteins remained after the water molecules were removed from the crystal structures. Polar hydrogen was added to the protein structure according to a pH of 7.4 using PDB2PQR Server, version 2.0.0. The grid box was centred on the receptor and covered the entire receptor. The docking was carried out using AutoDock Vina 1.1.2, the conformations displaying the highest binding affinity (the more negative value) were chosen as the best-docked model. The docking outputs were analysed with Ligplot<sup>+</sup> software using default parameters. The Ligplot<sup>+</sup> software produced a 2-dimensional (2D) diagram of the protein–ligand complex interaction with residue involved in the binding and type of bonding. The 3D superimposed diagram of the complex binding pose was created using PyMOL™ 1.7.4 software.

## 3. Results

### 3.1. Melanoma cytotoxicity evaluation

Table 1 shows the median inhibitory cytotoxicity activity (IC<sub>50</sub>) of different PB extracts prepared using different concentrations of methanol and water ratios. The data revealed that the IC<sub>50</sub> on A375 was solvents' polarity dependent with A > B > C > D > E. Additionally, D and E showed to have higher cytotoxicity activity compared to the remaining with the IC<sub>50</sub> value < 50 µg/mL viz. 39.8 and 27.8 µg/mL, respectively.

**Table 1**

Median inhibitory concentration (IC<sub>50</sub>) anticancer activity of PB extracts.

Extract	Concentration of methanol: water (%)	Median concentration (µg/mL)
A	0:100	100.9 ± 5.3
B	75:25	76.2 ± 4.7
C	50:50	53.7 ± 2.3
D	25:75	39.8 ± 2.1
E	100:0	27.8 ± 3.6

Data expressed as mean ± SD (n = 5).

### 3.2. Bioactive profiling using GC–MS

The identified putative bioactive through GC–MS analysis were found to be malic acid, galactitol, citric acid, palmitic acid, cholest-7-en-3beta-ol, 4,4-dimethyl-, acetate, gallic acid, linoleic acid, stearic acid, 4-androsten-4-ol-3,17-dione and isolongifolol. The putative bioactive compounds are labelled in Fig. 1 and the details of these compounds are reported in Table 2. Fig. 1 shows different concentrations of methanol: water that plays an essential role in extracting bioactive compounds from PB. The most prominent bioactive compound namely 4-androsten-4-ol-3,17-dione was found to be present in all types of solvents at high intensity. As the polarity of the solvents decreased, palmitic acid, cholest-7-en-3beta-ol, 4,4-dimethyl-, acetate linoleic acid, stearic acid and isolongifolol intensity started to increase. On the contrary, as polarity of the solvent decreased, malic acid, galactitol, gallic acid and citric acid intensity started to decline.

### 3.3. Multivariate data analysis

The MVDA correlated cytotoxicity activity (IC<sub>50</sub>) with GC–MS data, which discriminated compounds identified through GC–MS and developed an orthogonal partial least square (OPLS) model. The OPLS model differentiated mass to charge ratio (*m/z*) of specific retention time (OPLS component 1) as x variables and the IC<sub>50</sub> values (OPLS component 2) as y variable. The OPLS model calculated and discriminated the components to pinpoint the *m/z* which contributed to the activity. The OPLS model developed reliability which was evaluated through parameters of goodness of fit, permutation test, and model's ability to predict y value (Murugesu et al., 2018). Fig. 2 (A) presents the scatter plot based on the GC–MS detected compounds profile and cytotoxicity activity (IC<sub>50</sub> value) of the PB extracts. The most active samples namely E and D with IC<sub>50</sub> values < 30 µg/mL and 45 µg/mL were observed in the positive quadrant. On the other hand, less active samples namely C, B and A were distributed at the negative quadrant. The summary of the fit plot displayed the cumulative R<sub>2</sub> and Q<sub>2</sub> for the Y-matrix modelled by X. Fig. 2 (B) presents a summary of fit for GC–MS metabolites OPLS model. The OPLS component 1 explained 59% of the variation, while OPLS component 2 explained 29.3%.

Using a permutation test of the observed versus predicted plot, the developed OPLS model was validated. The permutation test shown in Fig. 3(A) gave intercepts 1/7 fraction from the total sum of the square of intercept Y-Value and predicted the model intercept Y-value. The goodness of fit (R<sup>2</sup>Y) and predictive ability (Q<sup>2</sup>Y) value for the OPLS model using GC–MS data in this study was found to be acceptable when the values of both R<sub>2</sub>Y and Q<sub>2</sub>Y were calculated as 0.14 and –0.304, respectively (Saleh et al., 2018). Fig. 3(B) presents a loading scatter plot of different concentrations of methanol: water of PB extracts. The points indicate metabolites identified from PB methanol: extract (E) and the labelled metabolites indicate the compounds identified as effective

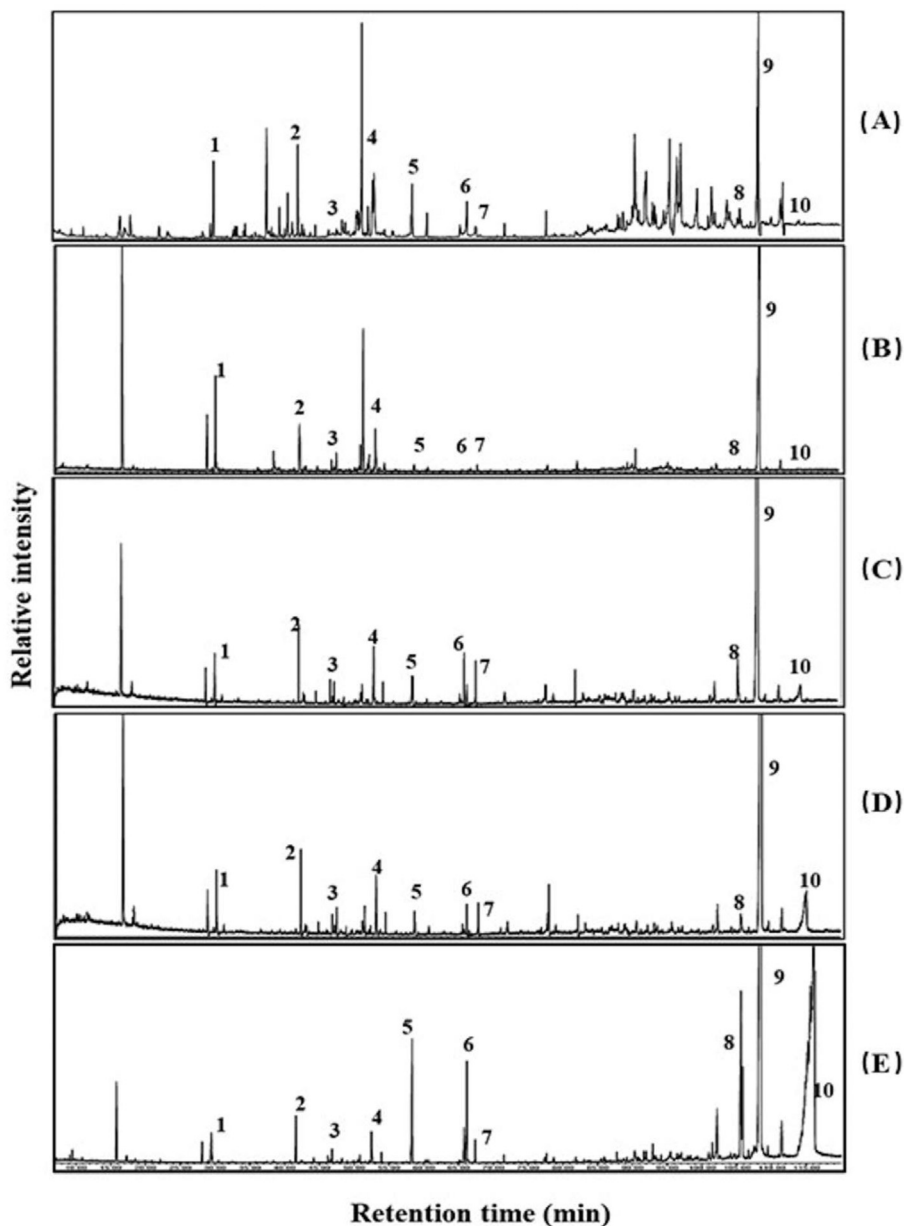


**Fig. 1.** GC-MS chromatogram of metabolites in 0% (A), 25% (B), 50% (C), 75% (D) and 100% (E) of methanol: water dilution of PB extract. (1) malic acid, (2) galactitol, (3) citric acid, (4) gallic acid, (5) palmitic acid, (6) linoleic acid, (7) stearic acid, (8) cholest-7-en-3beta-ol, 4,4-dimethyl-, acetate, (9) 4-androsten-4-ol-3,17-dione and (10) isolongifolol.

**Table 2**

Tentative compounds detected in the PB extracts via GC-MS analysis.

No	Retention time (min)	PA (%)	Similarity index	M <sup>r</sup>	MF	TM
1	28.11	0.31	90	134.08	C <sub>4</sub> H <sub>6</sub> O <sub>5</sub>	Malic acid
2	41.63	0.66	89	182.17	C <sub>6</sub> H <sub>14</sub> O <sub>6</sub>	Galactitol
3	46.22	0.15	94	192.12	C <sub>6</sub> H <sub>8</sub> O <sub>7</sub>	Citric acid
4	53.93	0.21	96	170.12	C <sub>7</sub> H <sub>6</sub> O <sub>5</sub>	Gallic acid
5	58.14	1.55	96	256.24	C <sub>16</sub> H <sub>32</sub> O <sub>2</sub>	Palmitic acid
6	65.75	1.63	90	280.45	C <sub>18</sub> H <sub>32</sub> O <sub>2</sub>	Linoleic acid
7	66.04	0.27	92	284.48	C <sub>18</sub> H <sub>36</sub> O <sub>2</sub>	Stearic acid
8	104.72	4.12	90	428.7	C <sub>31</sub> H <sub>52</sub> O <sub>2</sub>	Cholest-7-en-3beta-ol, 4,4-dimethyl-, acetate
9	108.43	29.20	95	302.4	C <sub>19</sub> H <sub>26</sub> O <sub>3</sub>	4-Androsten-4-ol-3,17-dione
10	116.00	5.11	93	222.4	C <sub>15</sub> H <sub>26</sub> O	Isolongifolol

MF = molecular formula, PA = peak area, TM = tentative metabolites, H = hydrogen, C = Carbon and O = oxygen.

in exhibiting cytotoxic activity on A375 cells. The potential active compounds identified were 4-androsten-4-ol-3,17-dione, cholest-7-en-3beta-ol, 4,4-dimethyl-, acetate, gallic acid and isolongifolol. The compound's structure is shown in Fig. 4.

### 3.4. Molecular interaction of target compounds with Bcl-2 protein

The study evaluated molecular interaction of the four ligands identified through GCMS analysis with anticancer targets, *Homo*

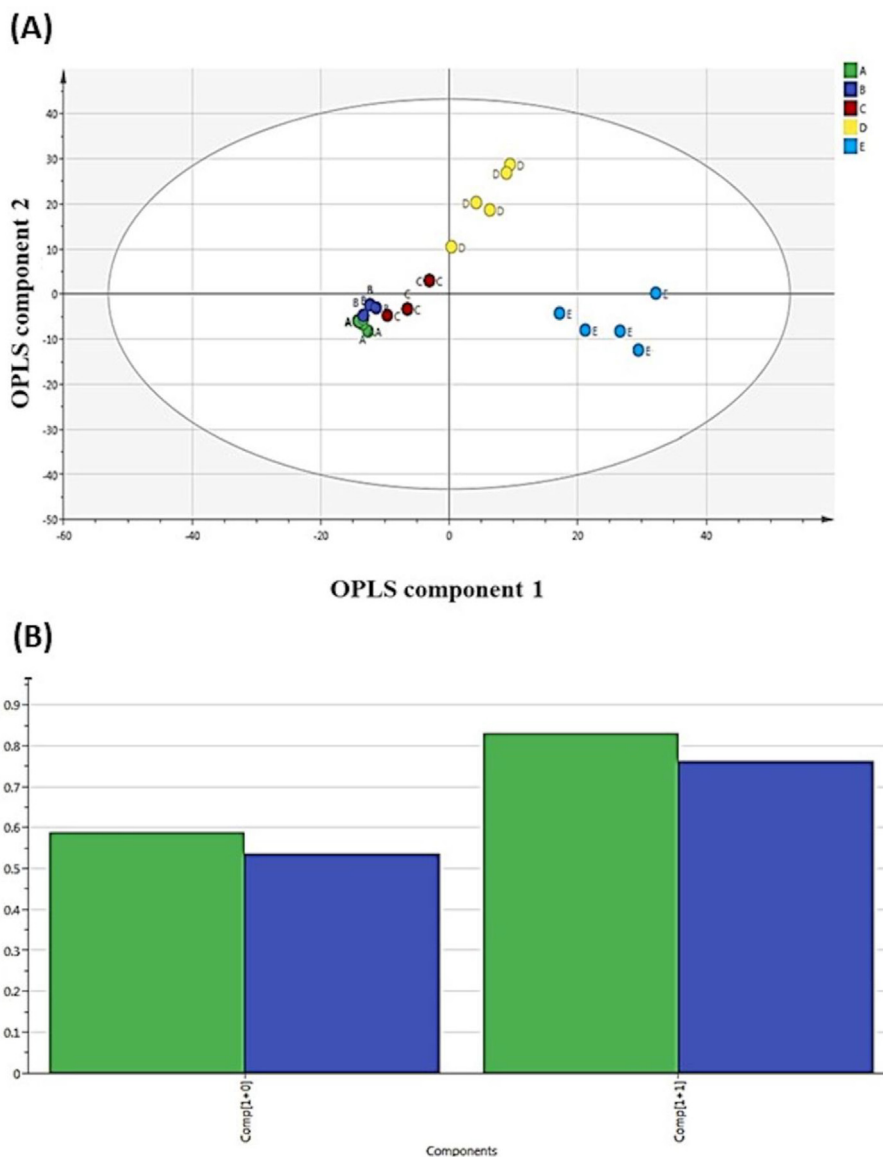


**Fig. 2.** Multivariate analysis based on OPLS model of PB extracts (A, B, C, D and E) obtained using GC-MS. (A) The score plots. (B) The summary of fit.

*sapiens* Bcl-2 and cyclin B/CDK1 complex. The binding affinities and 2D molecular interaction between ligands and Bcl-2 are presented in Table 3 and supplementary file. Lower value indicates higher binding affinity and favorable binding interaction. Table 3 reveals Bcl-2 receptor, namely navitoclax exhibited highest binding affinity with  $-11.5$  kcal/mol by forming hydrophobic interaction with VAL118, VAL115, SER75, GLU119, ASN122, ASP62, LEU160, VAL107, TYR161, PHE63, ALA59, ALA72, ARG65, TYR67 residues and six hydrogen bonds with five residues namely ARG68, ARG66, SER64, LYS22 and ARG26. Among the four identified compounds, cholest-7-en-3beta-ol, 4,4-dimethyl-, acetate showed the highest binding affinity ( $-8.7$  kcal/mol). The binding of the compound towards Bcl-2 are dominated by hydrophobic contacts with 10 amino acid residues include TYR161, PHE63, ALA59, GLY104, TYR67, ARG65, ASP61, SER64, ARG66 and ASP62 residues due to its hydrocarbon skeleton. The second highest binding affinity was observed in the complex containing 4-androsten-4-ol-3, 17-dione and Bcl-2, with  $-8.4$  kcal/mol. The compound contains four fused rings with hydroxyl group (OH) and two carbonyl groups (C = O). The compound was predicted to make hydrophobic contact with 12 amino acids involving ARG65,

SER64, TYR67, ARG26, ARG66, LYS22, VAL118, VAL115, GLU119, PHE71, ARG68 and SER75 residues, as well as two hydrogen bonds with SER75 hydroxyl side chain and carbonyl backbone. The isolongifolol ( $-7.4$  kcal/mol) which contains a tricyclo was predicted to bind to Bcl-2 via 10 hydrophobic contacts with GLU111, PHE71, SER64, ARG68, SER75, ALA72, VAL115, VAL118, ARG26 and LYS22 residues. Additionally, it was also predicted to interact via its hydroxyl group to LYS22 and ARG26 of Bcl-2 to form two hydrogen bonds. Despite having the lowest binding affinity ( $-5.5$  kcal/mol), the hydroxyl group on gallic acid formed four hydrogen bonds with ARG86 and GLU138 residues. Moreover, seven hydrophobic contacts with TRP135, VAL193, ALA90, PHE89, TYR139, ARG86 and GLU138 residues were predicted to stabilise the ligand-receptor interaction.

### 3.5. Molecular interaction of target ligands with cyclin B/CDK1 complex protein

The binding affinities and 2D molecular interaction between the four identified compounds and cyclin B/CDK1 complex are presented in Table 4 and supplementary file. The control docking,

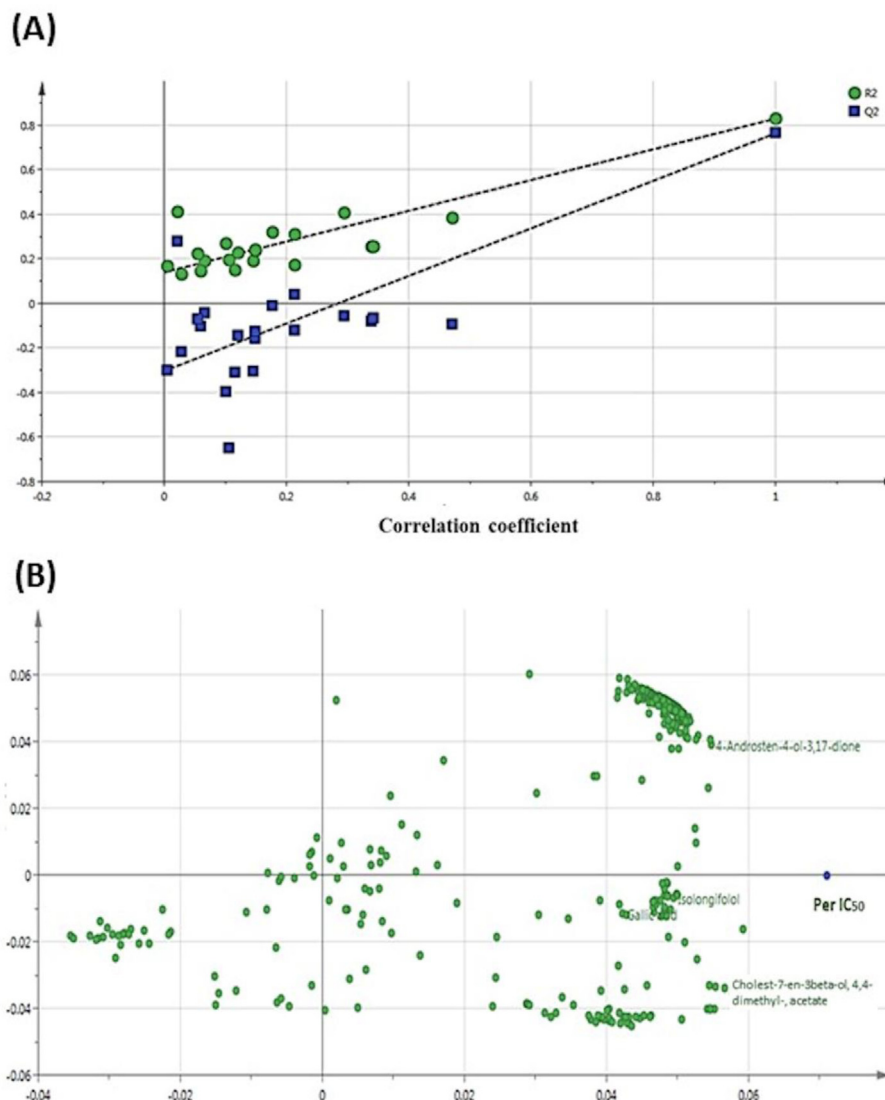


**Fig. 3.** Multivariate analysis based on OPLS model of PB extracts (A, B, C, D and E) obtained using GC–MS (A) Permutation of the OPLS model. The intercept of the fraction of the total sum of the squares ( $R^2$ ) was 0.185 while the intercept of the predictive ability ( $Q^2$ ) of the model was  $-0.304$ . (B) The loading scatter plot OPLS model of PB methanol extract using GC–MS.

namely flavopiridol, exerted a high binding score of  $-9.6$  kcal/mol. Its ketone group formed a hydrogen bond with LEU83 and carbons from flavopiridol aided hydrophobic contact with ALA31, LEU135, PHE80, VAL64, ASP146, TYR15, VAL18, MET85, ILE10, GLY11, PHE82 residues. Cholest-7-en-3beta-ol, 4,4-dimethyl-, acetate demonstrated comparable binding affinity to that of flavopiridol with the binding affinity of  $-9.5$  kcal/mol. The binding of cholest-7-en-3beta-ol, 4,4-dimethyl-, acetate was mainly dominated by hydrophobic contacts due to four fused ring skeleton and alkyl substituent which is hydrophobic in nature. This leads to a formation of 15 hydrophobic contacts with SER84, LYS89, MET85, LEU83, LEU135, ALA31, VAL18, ALA145, GLU51, PHE80, LYS33, ASP146, VAL64, ILE10 and ASP86 residues. The docked complex of 4-androsten-4-ol-3,17-dione and the protein with the binding score of  $-8.8$  kcal/mol revealed that its binding affinity was largely attributed by the interaction with GLY11, TYR15, ASP86, VAL64, ALA145, PHE80, LYS33, VAL18, ILE10 and ASP146 residues. Furthermore, a hydrogen bond was found to form between the carbonyl group of 4-androsten-4-ol-3,17-dione and ASP146 residue. In isolongifolol docked complex ( $-8.6$  kcal/mol), it was predicted that the hydroxyl group formed two hydrogen bonds with

THR329 and MET335, while the carbon backbone contributed majorly in the complex interaction with 11 hydrophobic interactions between its carbon and PHE338, VAL336, ILE343, VAL226, TYR223, ASP230, PRO301, SER227, PRO340, MET335 and THR329 residues. As for gallic acid which showed the moderate binding score of  $-7.1$  kcal/mol, a total of eight hydrophobic interactions with residues at the binding site was predicted, namely ILE343, SER227, VAL226, VAL336, MET335, THR329, MET330 and ARG201. In addition, gallic acid also formed eight hydrogen bonds between three hydroxyl groups with PHE338, MET335, THR329, MET330 and ARG201 residues to assist its binding to the protein. Overall, the docking findings showed that the hydrophobic interactions were more dominant in stabilizing the ligand-receptor complex.

Fig. 5 presents the location of binding sites of ligands in this study for Bcl-2 and cyclin B/CDK 1 complex proteins. Fig. 5 (A) reveals navitoclax, 4-androsten-4-ol-3,17-dione, cholest-7-en-3beta-ol, 4,4-dimethyl-, acetate and isolongifolol bind in the active site, suggesting the ligands might act as competitive inhibitor for Bcl-2. On the other hand, gallic acid was shown to bind far from the active site indicating its potential to influence the Bcl-2 inhibi-

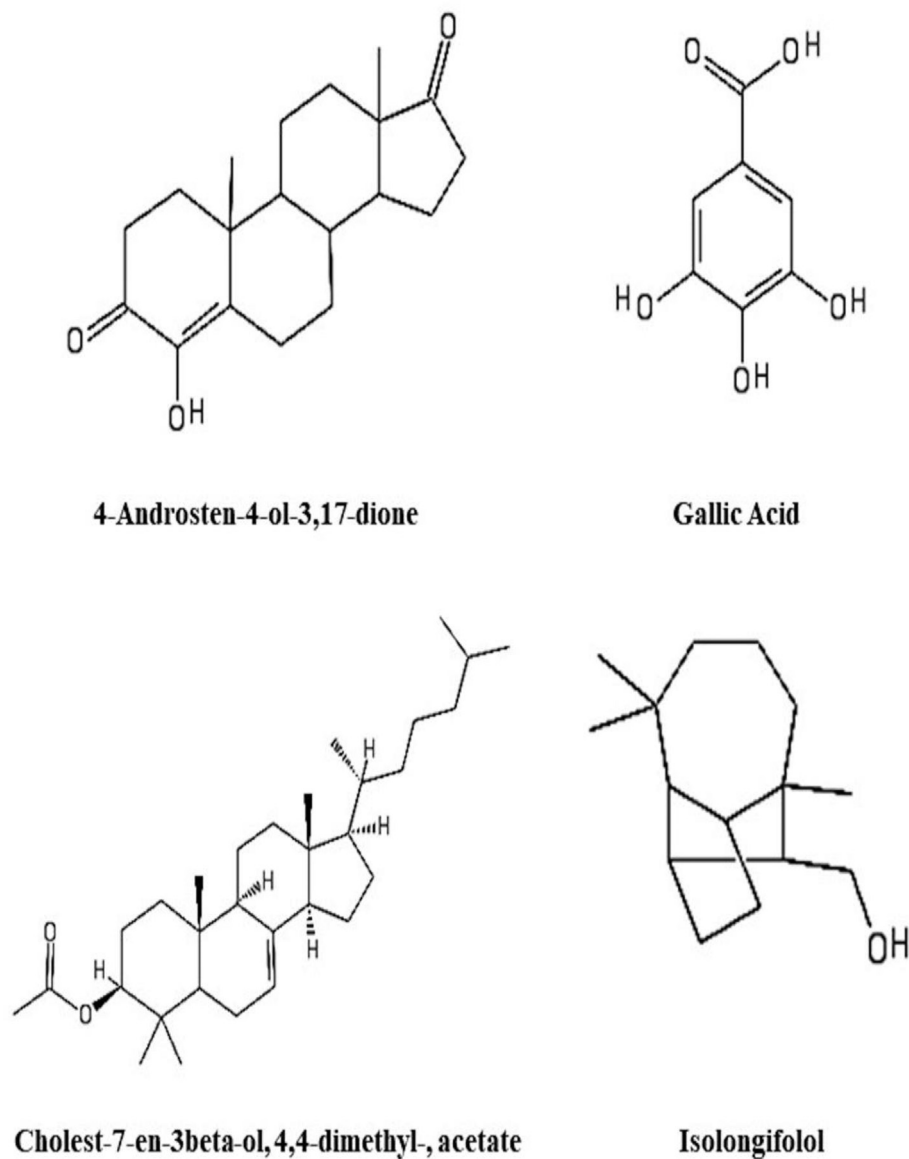


**Fig. 4.** Metabolites identified as potential putative active anticancer agents from PB methanol extract.

**Table 3**

Molecular interaction of Bcl-2 complex protein with the active ligands identified using GC-MS.

Ligand	Binding affinity (kcal/mol)	Residues assisting H-bond	Residues assisting hydrophobic contacts
Navitoclax (control)	-11.5	ARG68, ARG66, SER64, LYS22, ARG26	VAL118, VAL115, SER75, GLU119, ASN122, ASP62, LEU160, VAL107, TYR161, PHE63, ALA59, ALA72, ARG65, TYR67
4-Androsten-4-ol-3,17-dione	-8.4	SER75	ARG65, SER64, TYR67, ARG26, ARG66, LYS22, VAL118, VAL115, GLU119, PHE71, ARG68, SER75
Cholest-7-en-3beta-ol, 4,4-dimethyl-, acetate	-8.7		TYR161, PHE63, ALA59, GLY104, TYR67, ARG65, ASP61, SER64, ARG66, ASP62
Gallic acid	-5.5	ARG86, GLU138	TRP135, VAL193, ALA90, PHE89, TYR139, ARG86, GLU138
Isolongifolol	-7.4	ARG26, LYS22	GLU111, PHE71, SER64, ARG68, SER75, ALA72, VAL115, VAL118, ARG26, LYS22

tion via a non-competitive mode. As for cyclin B/CDK 1 complexes, the ligands demonstrated binding preference on two different binding sites as shown in Fig. 5 (B). The identified compound 4-androsten-4-ol-3,17-dione, cholest-7-en-3beta-ol, 4,4-dimethyl-, acetate, and the control i.e. flavopiridol were observed to occupy

the active site, indicating that they follow the competitive inhibition. Meanwhile, isolongifolol and gallic acid were demonstrated to bind at an allosteric site. This indicates that they favours non-competitive binding in exerting cyclin B/CDK complex inhibition. In allosteric regulation, the compound that binds at a site other

**Table 4**  
Molecular interaction of cyclin B/CDK1 complex protein with the active ligands identified using GC-MS.

Ligand	Binding affinity (kcal/mol)	Residues assisting H-bond	Residues assisting hydrophobic contacts
Flavopiridol (control)	-9.6	LEU83	ALA31, LEU135, PHE80, VAL64, ASP146, TYR15, VAL18, MET85, ILE10, GLY11, PHE82
4-androsten-4-ol-3,17-dione	-8.8	ASP146	GLY11, TYR15, ASP86, VAL64, ALA145, PHE80, LYS33, VAL18, ILE10, ASP146
Cholest-7-en-3beta-ol, 4,4-dimethyl-, acetate	-9.5		SER84, LYS89, MET85, LEU83, LEU135, ALA31, VAL18, ALA145, GLU51, PHE80, LYS33, ASP146, VAL64, ILE10, ASP86
Gallic acid	-7.1	PHE338, MET335, THR329, MET330, ARG201	ILE343, SER227, VAL226, VAL336, MET335, THR329, MET330, ARG201
Isolongifolol	-8.6	MET335, THR329	PHE338, VAL336, ILE343, VAL226, TYR223, ASP230, PRO301, SER227, PRO340, MET335, THR329

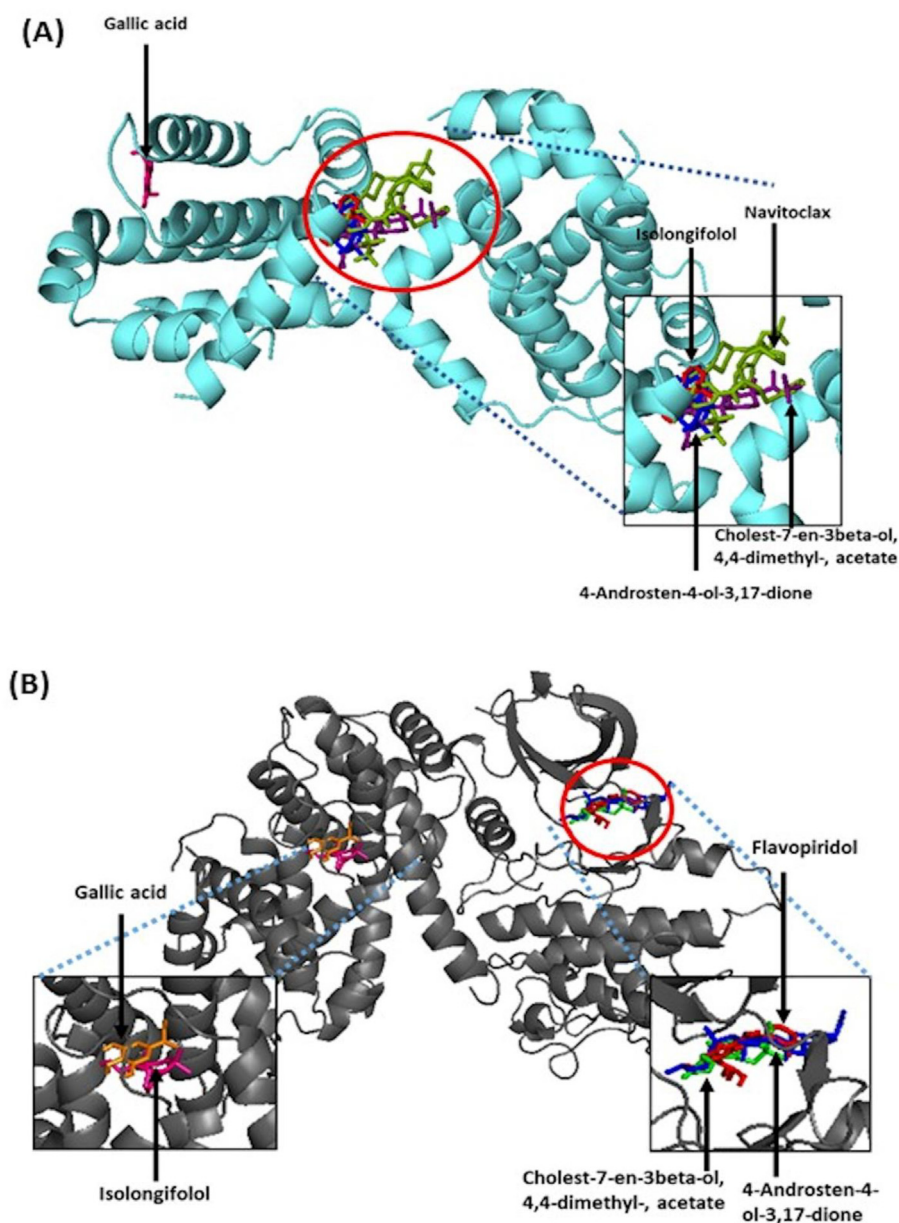


**Fig. 5.** Superimposed 3D diagram demonstrated the catalytic site of the control, 4-androsten-4-ol-3, 17-dione, cholest-7-en-3beta-ol, 4,4-dimethyl-, acetate, gallic acid and isolongifolol. A) Bcl-2 protein and B) cyclin B/CDK1 complex protein. The red circle indicates area of active site.

than the active site i.e., an allosteric site, changes and alters the enzyme in some way to make it inactive, hence, non-competitive inhibition.

#### 4. Discussion

Traditional medicine is the use of plant, animal, and mineral-based medicines, spiritual therapies, manual techniques, and exercises to cure, diagnose, and prevent sickness or preserve health (Fokunang et al., 2011). In developing and less developed countries, the usage of traditional and alternative medicine is common (Hill et al., 2019). In recent years, the PB had been reported to be used as alternative medicine for antioxidant, antiviral and anticancer purposes in Malaysia (Firus Khan et al., 2019a). Present study reports for the first time the evaluation of PB extract obtained through different methanol: water concentrations for cytotoxicity activity, characterization of the resultant extract using GC-MS metabolomics approach and elucidate the identified compounds interaction with targeted anticancer protein using molecular docking.

The cytotoxicity finding revealed the IC<sub>50</sub> on A375 was affected by the solvents polarity with E (methanol) was shown to have highest anticancer inhibitory activity compared to A (water). The result showed solvent polarity played an essential role in extracting compounds from extracts as water polarity index is 9 and methanol is 6.6 (Abarca-Vargas et al., 2016). Methanol was capable of extracting polar and non-polar compounds together from the PB, thereby suggesting the fact that the non-polar compounds present in PB might play an essential role in the anticancer activity. In addition, the finding was found in agreement with the GC-MS analysis in which compounds identified contained carboxyl (COOH), carbonyl (C = O) and hydroxyl (O-H) groups which will impart more polarity and hydrophilicity to the molecule and can be easily extracted with the polar solvents, for instance, malic acid, citric acid, gallic acid and galactitol all are considered polar molecules due to the presence of aforementioned polar functional groups. On the contrary, non-polar and semi-polar compounds viz. palmitic acid, linoleic acid, stearic acid, cholest-7-en-3beta-ol, 4,4-dimethyl-, acetate and 4-androsten-4-ol-3,17-dione with more C-H functional group as the carbon backbone in the structure will appear with increased intensity quantitatively as the solvents polarity decreases.

Through OPLS model of GC-MS-based metabolomics, 4 compounds were pinpointed their correlation with the cytotoxic activity on A375 cells namely gallic acid, isolongifolol, 4-Androsten-4-ol-3,17-dione and cholest-7-en-3beta-ol, 4,4-dimethyl-, acetate. Despite having been selected as possible bioactive compounds as anticancer agents in PB methanol extract, further literature on the bioactive compounds revealed for isolongifolol, 4-Androsten-4-ol-3,17-dione and cholest-7-en-3beta-ol, 4,4-dimethyl-, acetate that the anticancer effect for these compounds is yet to be reported. Gallic acid was reported to exert anticancer properties. Gallic acid is a natural phenolic compound found in several traditional medicinal plants or edible plant-based products, such as green tea, grapes, strawberries, bananas and many other fruits (Aborehab & Osama, 2019). Gallic acid has been reported to demonstrate anticancer activity against various types of cancers viz. lung, cervical cancer, lymphoblastic leukaemia, and hepatocellular carcinoma (Aborehab & Osama, 2019; Chen et al., 2017). Furthermore, gallic acid was reported in various studies to exhibit apoptosis through the mitochondria-mediated pathway as well as by activating the p53 pathway (Sun et al., 2016). Although the GC-MS MVDA suggested four compounds actively contributing to PB methanol anticancer activities on A375, remaining compounds namely linoleic acid (Diaz-Aragon et al., 2019), palmitic

acid (Pacheco et al., 2018), citric acid (Ren et al., 2017) and stearic acid (Ali Khan et al., 2013) identified in all solvents of PB extract have also been reported to exhibit anticancer activity. Therefore, the compounds detected in PB through GC-MS analysis in this study could also be responsible for the PB extract's an *in vitro* anticancer effect.

Since the identified active compounds are yet to be individually studied for their cytotoxic effect through any *in vivo* and *in vitro* assays, therefore molecular docking was performed to study the binding interaction between the active compounds (ligand) and targeted proteins (receptor) to understand their predicted anticancer potential. The results obtained in the form of binding affinity, binding pose and binding location clearly evidenced the potential interaction of the ligands to inhibit the protein's activity. The nature of a protein is dependent on amino acid side chain characteristics either hydrophobic, polar, acidic or basic, which will determine the type of folding the protein may exhibit (Pyrkov et al., 2010). The residues located in a ligand binding site may contribute to the binding affinity as the residue acts as conserved residue, catalytic nucleophile, catalytic electrophile, and many more to stabilise the receptor-ligand complex structure depending on the amino acids side chain (Raj & Poelarends, 2013).

The *Homo sapiens* anti-apoptotic protein Bcl-2 contains 288 residues that are arranged in four homology domains, namely BH1, BH2, BH3 and BH4. The protein consists of a hydrophobic binding groove, which accommodates the BH3 domain that is responsible for facilitating the interaction with anti-apoptotic protein and initiates the apoptosis cascade (Sathishkumar et al., 2012). Bcl-2 protein is composed of eight  $\alpha$  helix types of polypeptides where  $\alpha$ 2,  $\alpha$ 3,  $\alpha$ 4,  $\alpha$ 5,  $\alpha$ 7 and  $\alpha$ 8 hold the active site (Petros et al., 2004). Recent study on Bcl-2 structure reveals the presence of a secondary hydrophobic binding pocket which aids in ligand binding to maximise ligand interaction with Bcl-2 (Porter et al., 2009). Our molecular docking results showed that the four ligands namely navitoclax, 4-androsten-4-ol-3,17-dione, cholest-7-en-3beta-ol, 4,4-dimethyl-, acetate and isolongifolol were found to bind inside the active site, suggesting that these ligands may act as competitive inhibitors against Bcl-2 (Montero & Letai, 2018). Ligands viz. cholest-7-en-3beta-ol, 4,4-dimethyl-, acetate and 4-androsten-4-ol-3,17-dione interacted with the crucial active site residues at the BH3 groove, which aids in a small molecule to bind and prevent initiation of apoptosis cascade, namely ARG66 (Antony & Vijayan, 2016). In addition, the superimposed 3D diagram shown earlier anticipated that gallic acid preferred to bind to an allosteric regulation site enough to influence Bcl-2 inhibition via non-competitive mode.

From the ligand structure point of view, it can be deduced that the identified ligands are hydrophobic in the order of cholest-7-en-3beta-ol, 4,4-dimethyl-, acetate > 4-androsten-4-ol-3,17-dione > isolongifolol > gallic acid, as their structures mainly contain fused rings and aromatics backbone. However, gallic acid consists of aromatic structure, the ligand consists of a carbonyl functional group and hydroxyl group. Therefore, it tends to form hydrogen bonding in the binding site with nearby residues. From the ligand structure point of view, it can be deduced that the identified ligands and the compounds except gallic acid are fused ring compounds and mostly saturated in nature. Apart from the benzene ring, gallic acid bears more polar substituents i.e. carbonyl and hydroxyl groups that enable the compound to form hydrogen bonds with nearby residues. The hydrophobic interaction contributes majorly by carbons from aromatic structure of ligands as carbon is hydrophobic, which becomes the main drive force to segregate with surrounding (Brylinski, 2018). Furthermore, it can be deduced that hydrogen bonds formed between ligand functional groups (hydroxyl, carbonyl) and hydrophilic amino acid (ARG, SER, GLU) which aids in stabilising the complex (Pyrkov et al., 2010). Bcl-2

protein plays an essential role in inhibiting pro-apoptosis signals and promoting cell survival depending on the relative balance of pro and anti-apoptotic Bcl-2 protein (Correia et al., 2015). Agents/compounds/ligands bind in the BH3 binding groove of Bcl-2 inhibit Bcl-2 protein is also known as BH3 mimetics (Hata et al., 2015). The direct inhibition of Bcl-2 protein leads to overexpression of pro-apoptosis, namely Bax and Bak (Correia et al., 2015). Activating Bax and Bak is crucial in assembling into multimeric pores in the mitochondrial membrane to facilitate mitochondrial outer membrane permeabilisation (MOMP) and cytochrome c released into the cytosol (Kale et al., 2018). Cytochrome C in cytosol activates the caspase cascade hence resulting in apoptosis (Azman et al., 2014).

In our previous study, PBs extract induced cell cycle arrest in G2 phase, therefore, cyclin B/CDK1 complex was used in evaluating the cell cycle arrest mechanism (Firus Khan et al., 2019a,b). *Homo sapiens* cell cycle inhibitor, cyclin B/CDK1 complex is composed of chain A, chain B and chain C with 1184 residues. The CDK1-cyclin B protein structure consists of few parts, namely N-terminal lobe which is a twisted anti-parallel beta-sheet linked to C-terminal lobe of  $\alpha$ -helices via a flexible hinge sequence (Wood & Endicott, 2018) and the same protein structure comprises glycine-rich loop (sequence 1–36),  $\alpha$ -C-helix (residues 45–55), hinge (residues 80–84) and activation loop (residues 145–172). Furthermore, the active site of the protein is located in  $\alpha$ -L12 with LYS33, GLU51, and ARG150 residues at the active binding site (Shamsi & Shukla, 2020). Our superimposed 3D diagram shows the identified compounds bind to two locations. 4-androsten-4-ol-3,17-dione, cholest-7-en-3beta-ol, 4,4-dimethyl-, acetate, and the control docking flavopiridol bind inside the active site during the interaction. Interestingly, 4-androsten-4-ol-3,17-dione, cholest-7-en-3beta-ol, 4,4-dimethyl-, acetate was observed to interact with LYS33, which is one of the significant residues in the active site to inhibit cyclin B/CDK1 complex (Shamsi & Shukla, 2020). Whereas isolongifolol and gallic acid bind to an allosteric site interacting with residues on C-terminal lobe indicating non-competitive inhibitory effect.

The 4-androsten-4-ol-3, 17-dione and cholest-7-en-3beta-ol, 4,4-dimethyl-, acetate ligands contain cycloalkene and aromatic structure, hence the interaction between ligands and hydrophobic residues (VAL, PHE, LEU, ALA, GLY) resulting in the formation of hydrophobic interaction which contributed greatly for the high binding score. The binding affinity of both ligands was in line with hydrophobic order of the ligands, cholest-7-en-3beta-ol, 4,4-dimethyl-, acetate > 4-androsten-4-ol-3,17-dione > isolongifolol > gallic acid. Apart from forming hydrophobic interaction with non-polar amino acids, the ligands interacted with the polar amino acids as well, possibly to segregate from hydrophilic amino acids, stabilizing the complex. From our result, although gallic acid has the highest number of hydrogen bonds formed, its binding affinity is the weakest. This suggests the hydrophobic nature of the allosteric site. Cell growth is controlled through cell cycle regulatory mechanisms which determines whether an individual cell undergoes cell proliferation or apoptosis (Xu et al., 2011). Cyclin/CDK family regulates each phase and for progression from G2 to M phase, cyclin B/CDK1 complex activation is necessary. Cyclin B/CDK1 complex catalysis at G2/M checkpoint initiates cells to enter the mitotic phase from G2 phase (Lindqvist et al., 2007). In G2 phase, cyclin B level rises which allows accumulation of the cyclin B-CDK1 protein complexes, however in this stage, the complexes get inactivated due to phosphorylation of WEE1 and MYT1 kinases (Chow et al., 2011). At the end of the G2 phase, the inactive cyclin B/CDK1 complexes are activated by CDC25 and inactivate the WEE1/MYT1 simultaneously, hence allowing entry into the mitosis phase (Lindqvist et al., 2007). Direct inhibition of cyclin B/CDK1

binding, or activation disrupts the M phase entry, thereby causing the cell to arrest in G2 phase (Potapova et al., 2009).

## 5. Conclusion

Present study is the first study to report PB extract characterization using the metabolomics approach and evaluate the identified putative active compounds anticancer activity with selected protein to explain its mechanism using molecular docking. The PB extracts were subjected to the characterization using GC-MS based metabolomics approach to identify putative anticancer agents of PB. The E extract (methanol) revealed the highest inhibitory activity. Four compounds in E extract namely cholest-7-en-3beta-ol, 4,4-dimethyl-, acetate (1), 4-androsten-4-ol-3,17-dione (2), isolongifolol (3) and gallic acid (4) were identified as potential anticancer agents. The *in-silico* evaluation with Bcl-2 and cyclin B/CDK1 complex revealed, the lowest binding affinity as cholest-7-en-3beta-ol, 4,4-dimethyl-, acetate < 4-androsten-4-ol-3,17-dione < isolongifolol < gallic acid in inhibiting both proteins. In addition, hydrophobic interaction was found to dominate the ligand-protein interaction in both target proteins. The overall findings in present study provide constructive evidence for future research in evaluating these compounds individually for anticancer effect instead of using whole PB.

## Declaration of Competing Interest

The authors declare that they have no known competing financial interests or personal relationships that could have appeared to influence the work reported in this paper.

## Acknowledgement

This work was funded by Ministry of Higher Education (MOHE), Malaysia through FRGS 16-045-0544 and Researchers Supporting Project number (RSP2023R26), King Saud University, Riyadh, Saudi Arabia. Authors would also like to acknowledge the Department of Wildlife and National Parks Malaysia for approval to perform this study.

## References

- Abarca-Vargas, R., Peña Malacara, C., Petricevich, V., 2016. Characterization of Chemical Compounds with Antioxidant and Cytotoxic Activities in Bougainvillea x buttiana Holtum and Standl. (var. Rose) Extracts. *Antioxidants* 5 (4), 45. <https://doi.org/10.3390/antiox5040045>.
- Aborehab, N.M., Osama, N., 2019. Effect of Gallic acid in potentiating chemotherapeutic effect of Paclitaxel in HeLa cervical cancer cells. *Cancer Cell Int.* 19 (1), 1–13. <https://doi.org/10.1186/s12935-019-0868-0>.
- Ali Khan, A., Alanazi, A.M., Jabeen, M., Chauhan, A., Abdelhameed, A.S., 2013. Design, Synthesis and In Vitro Anticancer Evaluation of a Stearic Acid-based Ester Conjugate. *Anticancer Res* 33, 2517–2524.
- Antony, P., Vijayan, R., 2016. Acetogenins from *Annona muricata* as potential inhibitors of antiapoptotic proteins: A molecular modeling study. *Drug Des. Devel. Ther.* 10, 1399–1410. <https://doi.org/10.2147/DDDT.S103216>.
- Aziza, M.A., Ong, H.C., Vikineswary, S., Noorlidah, A., Haron, N.W., 2012. Ethnomedicinal resources used by the Temuan in Ulu Kuang village. *Studies on Ethno-Medicine* 6 (1), 17–22. <https://doi.org/10.1080/09735070.2012.11886415>.
- Azman, S., Zulkepli, N. A., & Abdul Wahab, R. 2014. Novel apoptotic regulators in carcinogenesis. In: *Novel Apoptotic Regulators in Carcinogenesis*. Springer Science+Business Media Dordrecht 2012. Doi: 10.1007/978-94-007-4917-7.
- Barroso, M.D.S., 2014. The Bezoar Stone: A Princely Antidote, The Távora Sequeira Pinto Collection – Oporto. *Acta Med. Hist. Adriat.* 12 (1), 77–98.
- Barroso, S., 2017. Chapter 11. Animal Stones and the Dark Age of Bezoars. In: *Toxicology in the Middle Ages and Renaissance*. Elsevier, pp. 115–123.
- Brylinski, M., 2018. Aromatic interactions at the ligand-protein interface: Implications for the development of docking scoring functions. *Chem. Biol. Drug Des.* 91 (2), 380–390. <https://doi.org/10.1111/cbdd.13084>.

- Chen, J., Ding, J., Wang, Z., Zhu, J., Wang, X., Du, J., 2017. Identification of downstream metastasis-associated target genes regulated by LSD1 in colon cancer cells. *Oncotarget* 8 (12), 19609–19630.
- Chow, J.P.H., Poon, R.Y.C., Ma, H.T., 2011. Inhibitory Phosphorylation of Cyclin-Dependent Kinase 1 as a Compensatory Mechanism for Mitosis Exit. *Mol. Cell Biol.* 31 (7), 1478–1491. <https://doi.org/10.1128/mcb.00891-10>.
- Correia, C., Lee, S.-H., Meng, X. W., Vincelettee, Nicole D, Knorr, Katherine L. B., Ding, H., Nowakowski, Grzegorz. S., & Dai, Haiming, Kaufmann, Scott. H. 2015. Emerging understanding of Bcl-2 biology: Implications for neoplastic progression and treatment. *Biochemistry Biophysical Acta*, 1853(7), 1658–1671. Doi: 10.1016/j.physbeh.2017.03.040.
- Diaz-Aragon, R., Ramirez-Ricardo, J., Cortes-Reynosa, P., Simoni-Nieves, A., Gomez-Quiroz, L.-E., Perez Salazar, E., 2019. Role of phospholipase D in migration and invasion induced by linoleic acid in breast cancer cells. *Mol Cell Biochem* 457 (1-2), 119–132.
- Duffin, C.J., 2013. Porcupine stones. *Pharm. Hist.* 43 (1), 13–22.
- Firus Khan, A.Y., Ahmed, Q.U., Narayanamurthy, V., Razali, S., Asuhaimi, F.A., Saleh, M.S.M., Johan, M.F., Khatib, A., Seeni, A., Wahab, R.A., 2019a. Anticancer activity of grassy Hystrix brachyura bezoar and its mechanisms of action: An in vitro and in vivo based study. *Biomedicine and Pharmacotherapy* 114. <https://doi.org/10.1016/j.biopha.2019.108841>.
- Firus Khan, A.Y., Asuhaimi, F.A., Jalal, T.K., Roheem, F.O., Natto, H.A., Johan, M.F., Ahmed, Q.U., Wahab, R.A., 2019b. Hystrix brachyura bezoar characterization, antioxidant activity screening, and anticancer activity on melanoma cells (A375): A preliminary study. *Antioxidants* 8 (2). <https://doi.org/10.3390/antiox8020039>.
- Fokunang, C.N., Ndikum, V., Tabi, O.Y., Jiofack, R.B., Ngameni, B., Guedje, N.M., Tembe-Fokunang, E.A., Tomkins, P., Barkwan, S., Kechia, F., Asongalem, E., Ngoupayou, J., Torimiro, N.J., Gonsu, K.H., Sielinou, V., Ngadjui, B.T., Angwafor, III, Nkongmeneck, A., Abena, O.M., Ngogang, J., Asonganyi, T., Colizzi, V., Lohoue, J., 2011. Traditional medicine: Past, present and future research and development prospects and integration in the national health system of Cameroon. *Afr. J. Tradit. Complement. Altern. Med.* 8 (3). <https://doi.org/10.4314/ajtcam.v8i3.65276>.
- Hata, A.N., Engelman, J.A., Faber, A.C., 2015. The BCL2 family: Key mediators of the apoptotic response to targeted anticancer therapeutics. *Cancer Discov.* 5 (5), 475–487. <https://doi.org/10.1158/2159-8290.CD-15-0011>.
- Hill, J., Mills, C., Li, Q., Smith, J.S., 2019. Prevalence of traditional, complementary, and alternative medicine use by cancer patients in low income and lower-middle income countries. *Glob. Public Health* 14 (3), 418–430. <https://doi.org/10.1080/17441692.2018.1534254>.
- Kale, J., Osterlund, E.J., Andrews, D.W., 2018. BCL-2 family proteins: Changing partners in the dance towards death. *Cell Death Differ.* 25 (1), 65–80. <https://doi.org/10.1038/cdd.2017.186>.
- Lim, N.T., Wang, D., 2016. Records of the Malayan porcupine, *Hystrix brachyura* (Mammalia : Rodentia : Hystricidae) in Singapore. *Nature in Singapore* 9 (August), 63–68.
- Lindqvist, A., Van Zon, W., Rosenthal, C.K., Wolthuis, R.M.F., 2007. Cyclin B1-Cdk1 activation continues after centrosome separation to control mitotic progression. *PLoS Biol.* 5 (5), 1127–1137. <https://doi.org/10.1371/journal.pbio.0050123>.
- Lunde, D., Aplin, K., Molur, S., 2008. *Hystrix brachyura*, Malayan Porcupine. In International Union for Conservation of Nature Vol. T10749A321. <https://doi.org/10.2305/IUCN.UK.2008.RLTS.T10749A321.2358>.
- Manier, S.K., Keller, A., Schäper, J., Meyer, M.R., 2019. Untargeted metabolomics by high resolution mass spectrometry coupled to normal and reversed phase liquid chromatography as a tool to study the in vitro biotransformation of new psychoactive substances. *Sci. Rep.* 9 (1), 1–11. <https://doi.org/10.1038/s41598-019-39235-w>.
- Montero, J., Letai, A., 2018. Why do BCL-2 inhibitors work and where should we use them in the clinic? *Cell Death Differ.* 25 (1), 56–64. <https://doi.org/10.1038/cdd.2017.183>.
- Murugesu, S., Ibrahim, Z., Ahmed, Q., Yusoff, N.N., Uzir, B., Perumal, V., Abas, F., Saari, K., 2018. Clinacanthus nutans Lindau Leaves by Gas Metabolomics and Molecular Docking Simulation. *Molecules* 23 (2402), 1–21. <https://doi.org/10.3390/molecules23092402>.
- Pacheco, B.S., dos Santos, M.A.Z., Schultze, E., Martins, R.M., Lund, R.G., Seixas, F.K., Colepicolo, P., Collares, T., Paula, F.R., De Pereira, C.M.P., 2018. Cytotoxic activity of fatty acids from Antarctic macroalgae on the growth of human breast cancer cells. *Front. Bioeng. Biotechnol.* 6 (DEC), 1–10. <https://doi.org/10.3389/fbioe.2018.00185>.
- Petros, A.M., Olejniczak, E.T., Fesik, S.W., 2004. Structural biology of the Bcl-2 family of proteins. *Biochimica et Biophysica Acta - Molecular Cell Research* 1644 (2–3), 83–94. <https://doi.org/10.1016/j.bbamcr.2003.08.012>.
- Porter, J., Payne, A., de Candole, B., Ford, D., Hutchinson, B., Trevitt, G., Turner, J., Edwards, C., Watkins, C., Whitcombe, I., Davis, J., Stubberfield, C., 2009. Tetrahydroisoquinoline amide substituted phenyl pyrazoles as selective Bcl-2 inhibitors. *Bioorg. Med. Chem. Lett.* 19 (1), 230–233. <https://doi.org/10.1016/j.bmcl.2008.10.113>.
- Potapova, T., Daum, John. R., Byrd, Kendra. S., Gorbsky, Gary. J., 2009. Fine Tuning the Cell Cycle: Activation of the Cdk1 Inhibitory Phosphorylation Pathway during Mitotic Exit. *Mol. Biol. Cell* 20, 1737–1748. <https://doi.org/10.1091/mbc.E08>.
- Pyrkov, T.V., Ozerov, I.V., Blitskaia, E.D., Efmov, R.G., 2010. Molecular docking: role of intermolecular contacts in formation of complexes of proteins with nucleotides and peptides. *Bioorg. Khim.* 36 (4), 482–492. <https://doi.org/10.1134/s1068162010040023>.
- Raj, H., Poelarends, G.J., 2013. The roles of active site residues in the catalytic mechanism of methylaspartate ammonia-lyase. *FEBS Open Bio* 3, 285–290. <https://doi.org/10.1016/j.fob.2013.07.002>.
- Ren, J.G., Seth, P., Ye, H., Guo, K., Hanai, J.I., Husain, Z., Sukhatme, V.P., 2017. Citrate Suppresses Tumor Growth in Multiple Models through Inhibition of Glycolysis, the Tricarboxylic Acid Cycle and the IGF-1R Pathway. *Sci. Rep.* 7 (1), 1–13. <https://doi.org/10.1038/s41598-017-04626-4>.
- Saleh, M. S. M., Siddiqui, M. J., Zaiton, S., & So, M. 2018. Correlation of FT-IR Fingerprint and  $\alpha$ -Glucosidase Inhibitory Activity of Salak (Salacca zalacca) Fruit Extracts Utilizing Orthogonal Partial Least Square. Doi: 10.3390/molecules23061434.
- Sathishkumar, N., Sathiyamoorthy, S., Ramya, M., Yang, D., Lee, H.N., Yang, D., 2012. Molecular docking studies of anti-apoptotic BCL-2, BCL-XL and MCL-1 proteins with ginsenosides from Panax ginseng. *J. Enzyme Inhib. Med. Chem.* 27 (5), 685–692. <https://doi.org/10.3109/14756366.2011.608663>.
- Shamsi, Z., Shukla, D., 2020. How does evolution design functional free energy landscapes of proteins? A case study on the emergence of regulation in the Cyclin Dependent Kinase family. *Mol. Syst. Des. Eng.* 5 (1), 392–400. <https://doi.org/10.1039/c9me00097f>.
- Sun, G., Zhang, S., Xie, Y., Zhang, Z., Zhao, W., 2016. Gallic acid as a selective anticancer agent that induces apoptosis in SMMC-7721 human hepatocellular carcinoma cells. *Oncol. Lett.* 11 (1), 150–158. <https://doi.org/10.3892/ol.2015.3845>.
- Wood, D.J., Endicott, J.A., 2018. Structural insights into the functional diversity of the CDK-cyclin family. *Open Biol.* 8 (9). <https://doi.org/10.1098/rsob.180112>.
- Xu, K., Liang, X., Wang, F., Xie, L., Xu, Y., Liu, J., Qian, X., 2011. Induction of G2/M phase arrest and apoptosis by potent antitumor APCA in human cervix carcinoma cells. *Anticancer Drugs* 22 (9), 875–885. <https://doi.org/10.1097/CAD.0b013e328349597d>.